The Editor's Choice

Akimichi Morita

Journal of Dermatological Science

VOLUME 65 NUMBER 3

A novel hairless mouse model for malignant melanoma

An animal model for malignant melanoma is a strong tool to develop biomarkers through the analysis of melanomagenesis. Thang et al developed a novel animal model that spontaneously develops malignant melanoma. They crossed oncogenic RET (RFP–RET)-carrying transgenic mice of line 304/B6 (RET-mice) with hairless mice (hr/hr) and newly established hairless RFP–RET-transgenic mice of line 304-hr/hr (HL-RETmice). The HL-RET-mice developed hyperpigmented skin and benign melanocytic tumors. Importantly, 63.8% (46/72) of the benign tumors were transformed to malignant melanoma in the HL-RET-mice. Mean time until the development of benign melanocytic tumors (2.4 months) in the HL-RET-mice was about half of that in the original RET-mice (4.6 months). Since early development of tumors could contribute to shortening of the research period, HL-RET-mice could be a useful model for analysis of melanomagenesis. The expression level of Mps one binder kinase activator-like-2B (Mobkl2b) in benign tumors was higher than that in malignant melanoma in HL-RET-mice. The author established a novel hairless RET-transgenic mouse line spontaneously developing cutaneous malignant melanomas from benign melanocytic tumors. This mouse model may be useful to find new candidates of melanoma-related molecule.

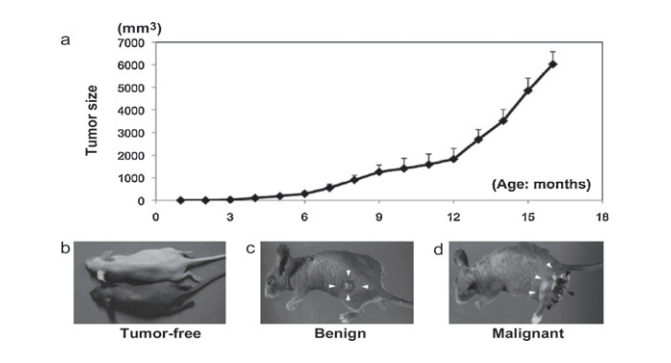

Time course of tumor growth and macroscopic appearance in HL-RET-mice. (a) Time course of tumor size in HL-RET-mice. (b) A control 1-month-old hairless mouse (b, top) and a littermate HL-RET-mouse with hyperpigmented skin (b, bottom). (c) A melanocytic benign tumor (white arrows) with hyperpigmented skin in a 6-month-old HL-RET-mouse. (d) An ulcerated malignant melanoma in a 14-month-old HL-RET-mouse.

Knocking-in the R142C mutation in transglutaminase 1 disrupts the stratum corneum barrier and postnatal survival of mice

Mutations in the gene encoding transglutaminase 1 (TG1) are responsible for various types of autosomal recessive congenital ichthyosis (ARCI), such as lamellar ichthyosis (LI), congenital ichthyosiform erythroderma (CIE) and some minor variants of ARCI. A point mutation of R143C in the Ð-sandwich domain of TG1 has been often identified in patients with LI or CIE. Nakagawa et al investigated the effect of that point mutation on skin barrier structures and functions and generated mice with a point mutation of R142C, which corresponds to the R143C mutation in human TG1. A mouse line with the R142C point mutation in TG1 was established using a gene targeting technique and the Cre-lox system. The skin phenotypes were analyzed in homozygous mutant Tgm1R142C/R142C mice. In the skin of Tgm1R142C/R142C mice, expression of the mutant transcripts was comparable with wild-type or Tgm1+/R142C mice. However, the amount of mutated protein in the skin was markedly decreased in Tgm1R142C/R142C mice, and the TG1 activity of Tgm1R142C/R142C keratinocytes was almost lost. The stratum corneum of those mice lacked cornified envelopes, and loricrin, the major structural component, failed to assemble at the corneocyte cell periphery. The intercellular lipid lamellar structures of the stratum corneum were irregular and the 13-nm periodic Xray diffractions from the stratum corneum

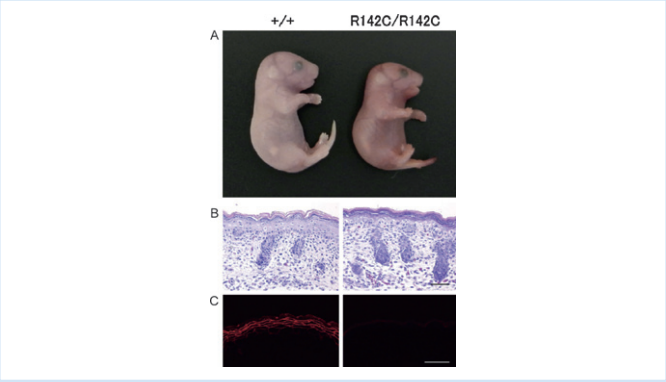

Macroscopic appearance and histology of 19.5-dpc wild-type (+/+) and Tgm1R142C/R142C mice (R142C/R142C).

lipid molecules were lost in vivo. The authors suggest that the R142C mutation of TG1 reduces the enzyme stability which is indispensable for development of the stratum corneum and skin barrier function and for postnatal survival of mice.

The predominant drug-specific T-cell population may switch from cytotoxic T cells to regulatory T cells during the course of anticonvulsant-induced hypersensitivity

Delayed hypersensitivity is responsible for severe cutaneous adverse drug reactions(cADRs), especially in Stevens-Johnson syndrome (SJS), toxic epidermal necrolysis, and drug-inducedhypersensitivity syndrome (DIHS). The drug-induced lymphocyte stimulation test (DLST), or lymphocyte transformationtest (LTT), is used to identify the culprit drug in severe cADR cases. Hanafusa et al examined the immune reactions in cADR patients through the identification of the drug-specific proliferating cells by flow cytometric DLST (FCM-DLST). The peripheral blood mononuclear cells of 16 anticonvulsant-induced cADR patients were investigated by conventional DLST and a FCM-DLST protocol in which CFSE dilution and BrdU incorporation were combined. In FCM-DLST, drug-specific proliferating T cells were detected as CFSElow BrdUhigh cells. Although CD4+ T-cell proliferation dominated the observed proliferation in most of the cases, drug-specific CD8+ cytotoxic T lymphocytes (CTLs) were detected, especially in the acute stages of the SJS case and one of the DIHS cases. FCM-DLST revealed that the cell proliferation detected by conventional DLST is a heterogeneous proliferation of both CD8+ CTLs and CD4+ T cells that likely includes Tregs. However, the number of cADR cases in this study was limited, which limits the conclusions that can be drawn from it.

Mcl-1 determines the imiquimod-induced apoptosis but not imiquimod-induced autophagy in skin cancer cells

Imiquimod had been shown to induce apoptosis and autophagy in several skin cancer cells, especially basal cell carcinoma (BCC) cells. Huang et al investigated the molecular mechanisms of imiquimod-induced apoptosis and autophagy in skin cancer cell lines. The mechanisms of imiquimod-induced decrease in Mcl-1 protein were evaluated by addition of cycloheximide, MG132 proteasome inhibitor or pancaspase inhibitor. The phosphorylation of eIF4E, 4E-BP1 and eEF2 in imiquimod treated cells were examined by immunoblotting. The imiquimod-induced apoptosis and autophagy were evaluated in Mcl-1-overexpressing cells by XTT test, mitochondrial membrane potential measurement, DNA content assay, LC3 immunoblotting, EGFP-LC3 puncta formation and quantification of acidic vesicular organelle with acridine orange staining. The decrease in the Mcl-1 protein level was faster and stronger than the decrease in Bcl-2 and Bcl-xL in imiquimod-treated skin cancer cells. The imiquimod-induced decrease in Mcl-1 protein was not caused by blocked transcription or the promotion of degradation but was associated with inactivation of translation factors in BCC cells. The Mcl-1-overexpressing BCC cells were more resistant to intrinsic cellular apoptosis than control BCC cells during imiquimod treatment. Mcl-1 overexpression in BCC cells resulted in the basal activation of autophagy but did not modulate imiquimod-induced autophagy or rescue imiquimod-induced autophagic cell death in BCC cells. The author concluded that Imiquimod may rapidly downregulate Mcl-1 protein levels by inhibiting translation in skin cancer cells. Mcl-1 may act to protect against apoptosis but not autophagy and autophagic cell death during imiquimod treatment in skin cancer cells.

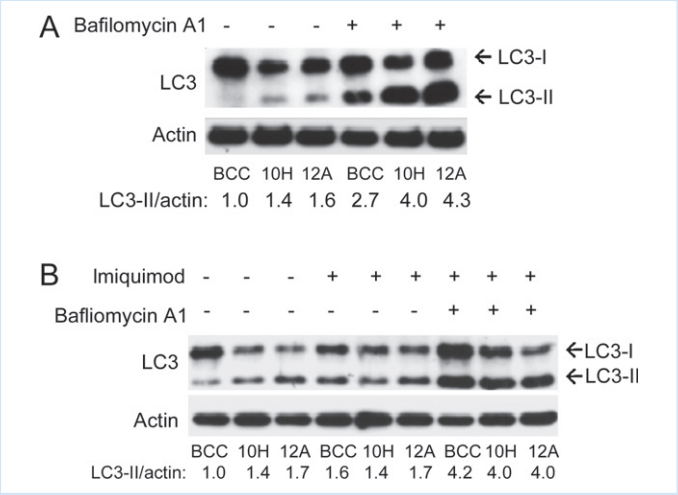

Mcl-1 overexpression enhances basal-level autophagy but cannot modulate imiquimod-induced autophagy in BCC cells.

The dimensions and characteristics of the subepidermal nerve plexus in human skin – Terminal Schwann cells constitute a substantial cell population within the superficial dermis

The skin constitutes the largest sensorial organ. Its nervous system consists of different types of afferent nerve fibers which spread out immediately beneath the skin surface to sense temperature, touch and pain. Reinisch et al investigated the dimension and topographic relationship of the different nerve fibers of the subepidermal nerve plexus in human hairy skin and to analyze numbers and marker expression of terminal Schwann cells. Nerve fibers and Schwann cells were investigated on dermal sheet preparations and thick sections of skin from various body regions. The dimension of subepidermal nerve fibers varied between different body sites with highest values in chest skin and lowest in posterior forearm skin. The majority of fibers (85.79%) were unmyelinated, thus representing C-fibers, of which 7.84% were peptidergic. Neurofilament-positive fibers (A-fibers) accounted for 14.21% and fibers positive for both neurofilament and myelin (Ab-fibers) for only 0.18%. The number of Schwann cells varied in accordance with nerve fiber length from 453 ±108 on chest skin to 184 ± 58/mm2 in skin of the posterior forearm. Terminal Schwann cells showed a marker profile comparable to Schwann cells in peripheral nerves with the notable exception of expression of NGFr, NCAM, L1CAM and CD146 on myelinating Schwann cells in the dermis but not in peripheral nerves. The author concluded that terminal Schwann cells constitute a substantial cell population within the papillary dermis and that both nerve fiber length and Schwann cell numbers vary considerably between different body sites.

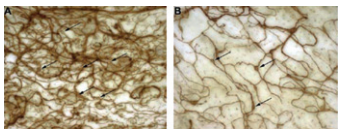

Depiction of the subepidermal nerve plexus by immunohistochemical staining for NGFr. A dense and regular nerve fiber network is visible in skin of the chest (A). In skin of the lower leg (B), the nerve plexus is regular as well, yet apparently less dense.

Epidermogenesis in a skin wound deep through the basement membrane contributes to scar formation

The basement membrane (BM) between the epidermis and dermis tightly connects the two compartments while preventing direct contact. During skin wound healing, a well-developed BM is not observed for a few months, which disrupts the homeostasis between the two compartments and allows abnormal epidermal–dermal events. Human amnion (AM) comprises a BM that is ultrastructurally and immunohistochemically similar to skin. Conventional living skin equivalents (LSEs) are made by seeding keratinocytes on fibroblast-embedded collagen gels without using amnion. AM-LSEs have a BM that clearly defines the dermal–epidermal junction with well-developed hemidesmosomes and a better-stratified epidermis with a more polarized, compactly aligned basal cell layer. Yang et al investigated the effects of epidermal–dermal interactions on scar formation during deep wound healing in LSEs and AM-LSEs. At 10 days, a new stratified and cornified epidermis filled the breached space of the wounded LSE. Immunohistochemical staining for keratin 10 and 16 revealed a less-differentiated, more activated neodermal phenotype compared with the unwounded LSE. TGF-Ð expression was up-regulated in the wounded area. Fibroblasts near or in contact with invading neoepidermis expressed Ð-smooth muscle actin, but the matrix far from the wound site did not. Activated keratinocytes secrete high levels of TGF-Ð1, which might induce myofibroblast differentiation. The authors concluded that altered skin homeostasis during epidermogenesis in wounded skin without a well-developed BM activates epidermis and myofibroblast differentiation, and contributes to scar formation.

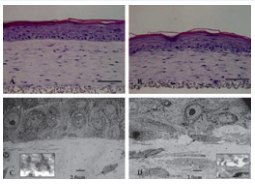

Histologic analysis (hematoxylin and eosin staining) (A and B) and ultrastructural analysis (transmission electron microscopy) (C and D) of an AM-LSE (A and C) and a conventional LSE (B and D). Compared to the conventional LSE, the AM-LSE shows a better stratified and polarized epidermis with a better-developed BM.